

“Influence of Initial Preform Aspect Ratios on the Densification Mechanism of Sintered Preforms of Iron and AISI 3115 P/M Steel during Hot Upset Forging”

Rajesh Reddy Koppula¹, K. S. Pandey²

¹Ex. M. Tech Student and ²Former Professor, Department of Metallurgical and Materials Engineering, National Institute of Technology Tiruchirappalli-620015, Tamil Nadu, India

Abstract: Hot upset forging experiments were carried out on sintered Iron and AISI 3115 Powder Metallurgy (P/M) steel preforms at $1120^{\circ}\pm 10^{\circ}\text{C}$ which were sintered at the same temperature for a period of sixty minutes. Present investigation, therefore, pertains to evaluate the effect of initial preform geometry on how the densification mechanism/s operate/s during hot upsetting mode. Preforms of initial aspect ratios of 0.6, 0.85 and 1.05 respectively were prepared on a 1.0 MN capacity Universal Testing Machine from Iron as well as from AISI 3115 composition powder blend using suitable die punch and bottom insert assembly in the pressure ranges of $537\pm 10\text{M Pa}$; $557\pm 10\text{M Pa}$; and $578\pm 10\text{MPa}$ respectively. With the control of pressure and powder weights, the initial compact densities were maintained in the range of 0.91 ± 0.01 of theoretical density. All compacts were coated with a thin film by using indigenously developed ceramic coating twice and at each time they were dried for a period of twelve hours under an ambient conditions. Ceramic coated compacts were sintered in an electric muffle furnace for a period of sixty minutes at $1120^{\circ}\pm 10^{\circ}\text{C}$. All sintered compacts except one from each aspect ratios were hot upset forged to different height strains and suitable plots were drawn between fractional theoretical density and the true height strains, true diameter strain and the true height strains, Poisson's ratio and the fractional theoretical density, the fractional theoretical density and the bulging ratio to establish empirical relations in the above said parameters. Analysis of the experimental and the calculated parameters along with the various plots have yielded several empirical relationships of practical as well as of theoretical importance.

Keywords: Aspect Ratio, Sintered Preforms, AISI 3115, Upset Forged, Densification, Poisson's Ratio, Bulging.

I. Introduction

Worldwide popularity of powder metallurgy (P/M) lies in the ability of this technique to produce complex metal shapes to exact dimensions, at high rates at extremely economical prices and providing much higher levels of technical achievements in quality [1]. P/M is at times the only manufacturing method that can be used for producing some materials such as porous materials, refractory metals and specially designed high duty alloys [2]. P/M processes possess the ability to produce net shape or near net shape high precision components with highest level of material utilization [3]. Therefore, the P/M processes compete with other methods on the basis of cost which can be lower for high volume production of complicated and intricate shaped components [3]. Further the sintered materials inherently possess high flexibility in their alloying design to increase their heat resistance and wear resistance in comparison with that of the conventionally produced wrought steels and cost alloys [2, 4]. The manufacturing processes for conventional P/M parts consist of powder production, blending (if the same is designed for the production of an alloy), compaction and finally sintering [5]. However, the sintered materials do contain inherent porosities whose presence have both beneficial as well as detrimental roles on the part performance [6]. Conventional P/M components are used in applications requiring low mechanical property levels [5]. In order to produce/prepare sound metallurgical structure, voids are to be eliminated or completely closed down. It is reported [6] that an increase in density would increase the strength, the fracture toughness and the resistance to crack growth. This can be achieved by secondary operations like forging, rolling, extrusion and extrusion forging etc. [7, 8]. Hot forging is generally employed to produce highly dense products by the P/M route. Powder preform forging involves the fabrication of preforms by the usual press and sinter processes followed by forging of the porous preforms into the final shapes [9]. Powder preform forging (PPF) has the advantages like optimum utilization, uniformity in properties, single blow finishing operation, improved weight control and savings in secondary machining operations [10]. The

basic process parameters such as forging temperature, initial preform density, alloying elements and the flow stresses do affect the density of the component/s after the forging operation is completed [10-13]. Therefore, a perfect combination of the above parameters for enhanced density is a must. Keeping this in mind Torre [14] considered porous metal as a metal containing a void for investigation of densification, i.e., a thick-walled sphere. According to him, the pressure required for the plastic deformation of a sphere containing a hole is given by:

$$P = 2\sigma_0 \ln (r_o/r_i) \dots \dots \dots (1)$$

Where, σ_0 = Flow stress of the material,
 r_o = Outside radius of the sphere,
 r_i = Hole radius (equal to the void radius), and,
 P = Pressure required to close down the pore.

Now, if the void radius is high, the pressure required to deform the sphere is substantially low. However, when the void radius approaches to zero, the pressure required to deform the sphere, i.e., then in this event in order to densifying the material becomes infinitely large. Therefore, it is, obvious that under the application of hydrostatic mode of loading, the void shape does not change, instead the size is reduced. The pore can be closed by applying the compression pressure (upsetting) which allows the material to flow freely in lateral direction, and, hence, the void becomes extremely flattened and elongated and the voids fragment into smaller voids. Since the shearing occurs along the interface of the opposite sides of the collapsed void, and, therefore, this would result in an increase in final density. It is reported [9] that the dynamic properties like fatigue and impact resistance depend not only on the residual porosity, but, also do depend, upon the characteristics of the metal flow during the densification mode. Hence, it is absolutely necessary to investigate the mechanism of material flow during metal preform hot upsetting.

In the present investigation, an attempt has been made to establish the densification mechanism/s and further to assess the influence of initial aspect ratios on the densification phenomenon during hot upset forging in a comprehensive manner. The materials used for the present study were Iron powder and AISI 3115 blend prepared from the elemental powders with the initial aspect ratios of 0.60, 0.85 and 1.05 respectively.

II. Experimental Details

2.1 Materials Required and Their Procurements

Iron powder of -180 μ m has been procured from M/s. The Sundaram Fasteners Limited, Hyderabad, Andhra Pradesh, India. The basic characteristic features of the Iron powder and the blend corresponding to AISI 3115 steel composition prepared from the elemental powders are given in Tables 1, 2, and 3 respectively. Suitable die set assembly was selected for compaction and the same one was made of High Carbon and High Chromium die steel. The assembly includes the mother die, the punch, the bottom insert, and the top and the bottom plates. These die parts have been machined from a suitable blanks of High Carbon and High Chromium steel, soaked in the temperature range of 950 \pm 10 $^{\circ}$ C for one hour to four hours depending upon the part keeping in mind that every 25mm diameter part was heated and soaked for one hour at the above temperature and quenched in oil. The hardness values were in the range of 59-61Rc. These parts were tempered to hardness values of 54-56Rc. Powder compaction was carried out on a 1.0MN capacity Universal Testing Machine. However, electric muffle furnace was used for sintering the compacts, which was kept near the Friction Screw Press of 1.0MN capacity to be used for forging operation. The material selected for the flat top and the bottom blocks of the forging hot dies was Molybdenum die steel and the each one of them having the dimensions of 240mmx150mmx100mm. The main alloying powders such as silicon, manganese, chromium, and nickel were procured from M/s. Grishma Enterprises, Mumbai, India. However, the graphite powder of 2 to 5 μ m was supplied by Ashbury Inc. New Jersey, USA exclusively for research purposes.

Table1 Selected Composition of AISI 3115 P/M Steel (Wt. %)

System	C	Si	Mn	Cr	Ni	Fe
AISI 3115	0.16	0.28	0.5	0.65	1.25	97.16

Table 2 Basic Characteristic of Iron Powder and AISI 3115 Powder Blend

Property	Iron	AISI 3115
Apparent Density, g/cc	2.877	3.349
Flow Rate(By Hall Flow meter), S/100g	57.520	56.37
Compressibility, g/cc at a Pressure of 480 \pm 10 MPa	6.751	6.757

Table 3 Sieve Size Analysis of Iron Powder

Sieve size (µm)	-180 +150	-150 +125	-125 +106	-106 +90	-90 +75	-75 +63	-63 +53	-53 +45	-45 +38	-38
Wt.% Ret.	0.019	0.115	0.046	0.048	0.184	3.505	26.090	25.24	2.249	42.469
Cum. Wt.% Ret.	0.019	0.134	0.180	0.228	0.412	3.917	30.007	55.247	57.496	99.965

2.2 Blending of Required Elemental Powders

Preparation of the powder blend of the AISI 3115 steel composition was carried out by taking accurately weighed elemental powders which can correspond to AISI 3115 composition as is given in Table 1 after sintering operation is completed. Elemental powders of the above requirements were taken and mixed in the stainless steel pot of the pot mill with a powder weight to ball weight ratio as 1.2:1. The lid of the pot was securely tightened and the pot was fixed on the pot mill and the mill was switched on. Immediately after the completion of every one hour of blending, nearly 100g of powder mix was taken and the flow rates and the apparent densities were measured. Once the above measurements were successfully completed, the tested powder mix was returned back to the pot and the pot's lid was securely tightened and the pot was re-fixed on the pot mill and the mill was switched on again. The above process was repeated thirty times or till the last three consecutive readings were consistently the same. Thus, the blending time arrived at was 30 hours, and, then the blending operation was discontinued. Now the powder blend was ready for compaction.

2.3 Compaction of Iron Powder and Blend of AISI 3115 P/M Steel Composition

Iron powder and the above prepared powder blend corresponding to AISI 3115 composition were accurately weighed and taken for the preparations of compacts with three initial aspect ratios, namely, 0.60, 0.85 and 1.05 respectively. Compacts of above initial aspect ratios were prepared on Universal Testing Machine of 1.0 MN capacity while using suitable die set assembly. In all, a total of 36 compacts were prepared. The compact densities were maintained in the range of 91±1 per cent of theoretical by applying the pressure in the range of 535±10 MPa for 0.60, 555±10MPa for 0.85 and 575±10MPa for 1.05 aspect ratios respectively. The diameter of the compaction die was 24.84^{+0.01} mm. Graphite powder with acetone as a paste was employed as a lubricant during compaction. The schematic diagram for powder compaction assembly is shown in fig.1.

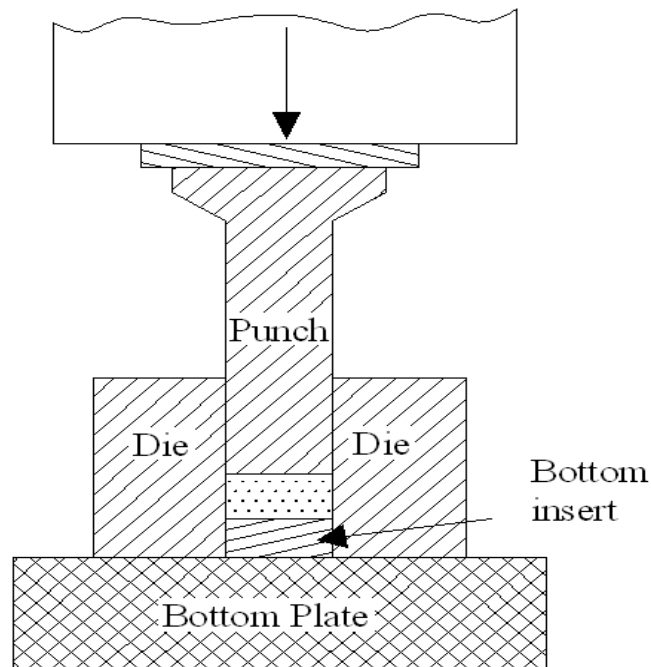


Figure 1 Schematic Diagram of Powder Compaction Assembly.

2.4 Application of Indigenously Developed Ceramic Coating

A thin film of indigenously developed ceramic coating [16] was applied on the entire surfaces of all the compacts to protect them against oxidation during sintering in the temperature range of 1120±10°C for a period of sixty minutes in an electric muffle furnace and subsequently transferring them to the bottom platen of the friction screw press for hot upset forging.

The ceramic coated compacts were recoated perpendicular to the previous coating and then both the coatings were allowed to dry under an ambient conditions for a period of twelve hours independently, i.e., one followed by the other after the completion of each coatings.

2.5 Sintering the Ceramic Coated Compacts of Iron Powder and AISI 3115 Powder Blend

Once the drying operation was completed, the ceramic coated compacts were kept in a ceramic tray and the tray was charged inside the uniform temperature zone of the electric muffle furnace. The furnace was switched on and the temperature was raised to $700^{\circ}\pm 10^{\circ}\text{C}$ and retained at this temperature for a period of 45 minutes in order to allow the volatile ingredients to be expelled out. Immediately after the completion of the pre-heating schedule, the furnace temperature was raised to $1120^{\circ}\pm 10^{\circ}\text{C}$, and, this temperature was retained for a period of sixty minutes. This completes the sintering schedule, and now the compacts are sintered and are ready for hot upset forging.

2.6 Hot Upset Forging

All sintered compacts except one of each aspect ratios, namely, 0.60, 0.85 and 1.05 and of each of the systems respectively were hot upset forged to different height strains on a 1.0MN capacity friction screw press on a Molybdenum hot flat steel dies. Immediately after hot upset forging of the sintered preforms were completed, the forged discs were quenched in linseed oil bath so as to retain the forged structures. Compacts of the each of the systems were separately sintered and separately forged in order to avoid the intermingling's of the forged discs of each of the systems.

2.7 Removal of Residual Ceramic Coatings from the Forged P/M Discs

Residual ceramic coatings if any was removed by mild machining/grinding or by mild filing or by using abrasive papers ensuring that no metal is abraded out. This procedure was employed to all the forged discs of both the systems and for all the three aspect ratios mentioned above. This adoption of removal of residual ceramic coating would bring uniformity as well as the accuracy in density measurements along with their actual forged dimensions.

2.8 Dimensional Measurements of Forged Discs and Sintered Preforms

Dimensions such as forged height (H_f), contact diameters [(top (D_{ct}), & bottom (D_{cb}))] and the bulged diameter (D_b) were accurately measured using digital Vernier calipers. A minimum of five readings were taken for each of the above parameters and then averaged out independently. Apart from the measurements of these parameters, initial height (H_o) and the initial diameter (D_o) of the sintered, but, thoroughly cleaned preforms were also measured by using the digital Vernier calipers. Now using these parameters, true height strain $\ln(H_o/H_f)$; true diameter strain $\ln(D_o/D_b)$; bulging ratio ($Br = \{D_b/D_o\}$) and $\log(D_b/D_o)$ were calculated and subsequently used to draw series of plots. Where, $D_c = \{(D_{ct} + D_{cb})/2\}$.

2.9 Density Measurements of Sintered and Forged Preforms

Density measurements of all the forged and sintered, but, cleaned compacts were found out by employing Archimedean principle [15]. Whereas, the density of sintered compacts were found out by calculating the volume geometrically and the mass in air using Adair-180 electronic balance with a sensitivity of 0.0001g. Prior to measuring the weights of the forged discs, a very fine film of a repellent oil [17] was applied on all the forged discs in order to avoid the penetration of water into the pores, thus, affecting true volume of the forged discs. The standard formula used to measure the density of the forged discs is given beneath:

$$\text{Density of the forged discs, } \rho_f, \text{ g/cc} = \{M_{\text{air}} / (M_{\text{air}} - M_{\text{water}})\} \times \rho_{\text{water}} \text{----- (2)}$$

Where, M_{air} = Mass in air, g; M_{water} = Mass in water, g, and, ρ_{water} = water density in g/cc.

Density correction was introduced depending upon the room temperature by using standard chart for density variations of water with respect to varying room temperature/s.

III. Results and Discussions

3.1 Deformation and Densification

Fig. 2 (a) has been drawn between fractional theoretical density (ρ_f/ρ_{th}) and the true height strain $\{\ln(H_o/H_f)\}$ obtained during hot forging of sintered iron powder preforms of different aspect ratios. This fig. very explicitly indicates that the lower aspect ratio (0.60 and 0.85) preforms densified comparatively at a much faster pace in contrast to the largest aspect ratio (1.05) preforms. However, the curve corresponding to initial preforms.

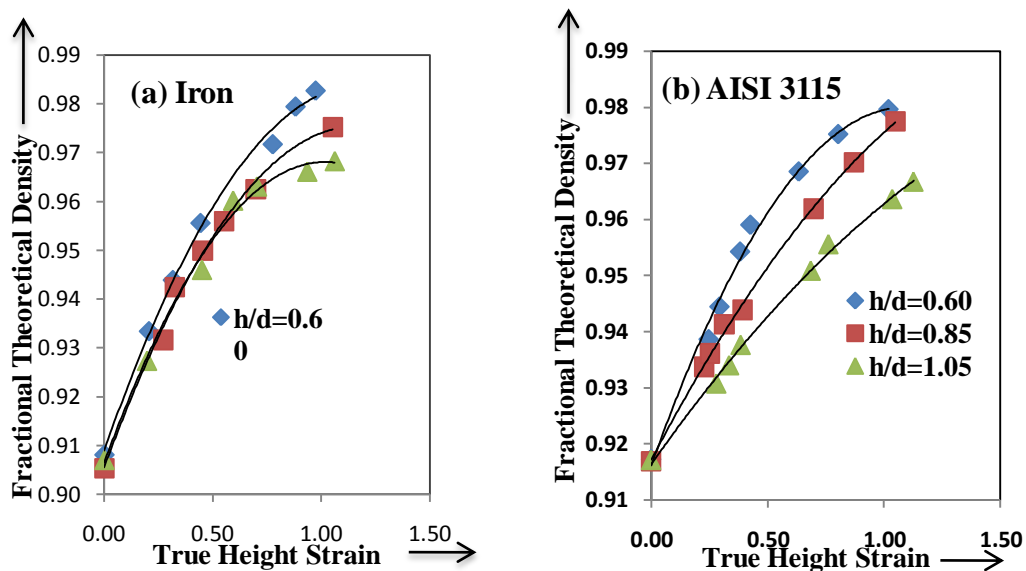


Figure 2 Relationship between the Fractional Theoretical Density and the True Height Strains during Hot Upset Forging of Sintered (a) Iron and (b) AISI 3115 P/M Steel Preforms

of aspect ratio of 0.85 positioned itself in between the curves corresponding to the lowest and largest aspect ratio preforms. In the initial stages of deformation, both the preforms, i.e., the largest and the medium sized densified with almost at the same pace up to the true height strains of 0.84 and there onwards the middle aspect ratio preforms densified at a faster rate compared to the largest aspect ratio preforms. This establishes that the largest aspect ratio preforms would always densify poorly compared to the lowest and the middle aspect ratio preforms which have shown much improved densification rates. Fig. 2 (b) has been drawn between fractional theoretical density attained and true height-strains during hot upset forging of sintered preforms of AISI 3115 P/M steel. This fig. very clearly shows that the densification rate shown by the lowest aspect ratio preforms have been maximum whereas the largest aspect ratio preforms exhibited the least rate of densification. This goes to establish that this AISI 3115 P/M steel is highly affected by the initial preform geometry during hot deformation and densification at $1120 \pm 10^\circ\text{C}$. The characteristic nature of curves shown in each of these figs. i.e., 2(a) and 2(b) are similar to each other, and, therefore, it is anticipated that all these densification curves would conform to a similar mathematical expression. Hence, the curve fitting techniques have been employed which resulted in yielding a second order polynomial to which all these curves conformed to. Thus, the densification curves shown through figs. 2(a) and 2(b) conformed to a second order polynomial of the form:

$$(\rho_f/\rho_{th}) = A_0 + A_1 \ln (H_0/H_f) + A_2 [\ln (H_0/H_f)]^2 \dots\dots\dots (3)$$

Where, ‘ A_0 ’, ‘ A_1 ’ and ‘ A_2 ’ are empirically determined constants found to depend upon the composition and the preform geometries. These constants are tabulated in Table-4. Observing these constants carefully it is found that the constant ‘ A_0 ’ is in very much close proximity to the initial preform density, and, therefore, did not contribute to densification. The values of the constant ‘ A_1 ’ is found to be positive and linearly multiplied to the true height strain, and, therefore, assisting to densification linearly. However, the values of the constant ‘ A_2 ’ is almost always negative and the same is multiplied to the square of the true height strain giving rise to a small negative value which can affect the density curves only in the final stages of deformation in such a manner so as to flatten the curves in last stages of deformation and densification. The observation that the lowest aspect ratio preforms densified at an enhanced pace compared to other larger aspect ratio preforms is justified because during the deformation, though percentage porosity content in the lowest and highest aspect ratio preforms are same, but, their effective depth of the pore bed in the lower aspect ratio preform is low, and, therefore, the load transfer along the direction of loading is quite quick and uniform. But, in larger aspect ratio preforms, the pore bed depth is comparatively higher, and, therefore, damping is on the higher side. Hence, the effective load transfer in the direction of loading is of lower magnitude in the larger aspect ratio preforms, and, therefore, results in poor densification in larger aspect ratio preforms. Further observing the Table-4, it is, found that the regression co-efficient, i.e., ‘ R^2 ’ values are in close proximity to unity indicating that the curve fittings have been carried out excellently well and accurate. Therefore, the above logistic discussion and the proposed densification equation of the second order polynomial stand the test of trial and are valid within the framework of the investigation.

Table 4 The Coefficients of the Second Order Polynomial of the Form $(\rho_f/\rho_{th}) = A_0 + A_1 \ln (H_0/H_f) + A_2 [\ln (H_0/H_f)]^2$ for Iron and AISI 3115 Steel during Hot Deformation.

System	Aspect Ratio	A ₀	A ₁	A ₂	R ²
Iron	0.6	0.906	0.122	-0.061	0.992
	0.85	0.904	0.138	-0.069	0.994
	1.05	0.906	0.138	-0.067	0.991
AISI 3115	0.6	0.915	0.12	-0.055	0.991
	0.85	0.916	0.086	-0.027	0.995
	1.05	0.916	0.06	-0.013	0.995

3.1 Relationship between True Diameter and True Height Strains

Figs. 3(a) and 3(b) have been drawn between the true diameter strains and true height strains for sintered Iron powder and AISI 3115 powder blend preforms during hot upset forging at 1120°±10°C respectively. Observing these two figs. 3(a) and 3(b) respectively, it is evident that all the data points remained below the theoretical line irrespective of the initial aspect ratios of the preforms and the compositions establishing very clearly that the values of the Poisson’s ratio would always remain less than 0.5. Further, it is observed that the data points corresponding to the lowest aspect ratio preforms always remained closer to the theoretical line except.

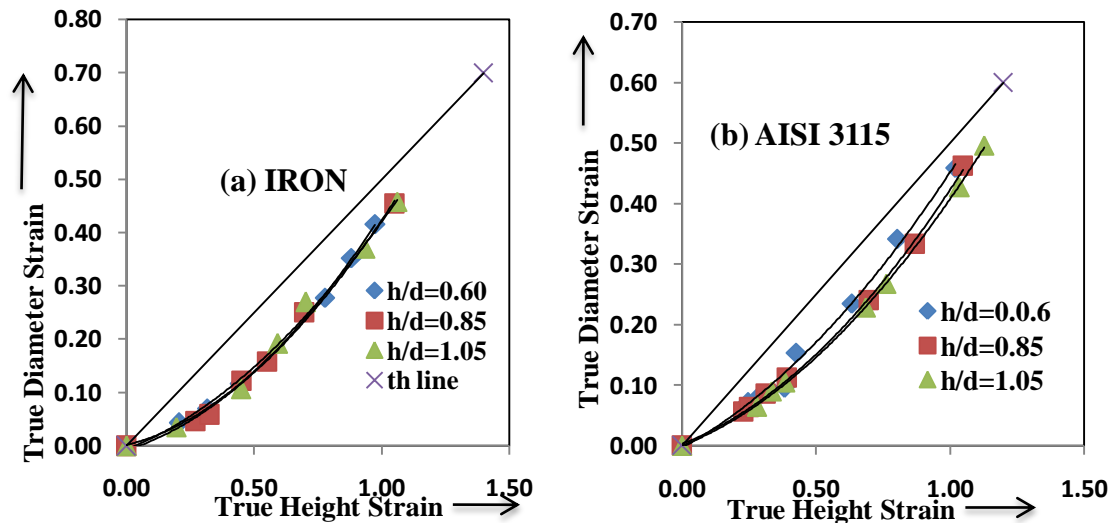


Figure 3 Relationship Between True Diameter Strain and True Height Strain During Hot Upset Forging of Sintered (a) IRON and (b) AISI 3115 Preforms.

In the case of iron powder preforms of all the aspect ratios, the data points lied in a very narrow band. It is further observed that the data points for largest aspect ratio preforms remained farthest away from the theoretical line. But, the data point corresponding to the middle aspect ratio (0.85) remained between the lowest and largest aspect ratio preforms. The curves drawn in figs. 3(a) and 3(b) are found to be quite similar to each other irrespective of the initial preform geometries and the systems compositions. Further it is established that the values of the Poisson’s ratios always remained less than one half. However, the critical analysis of these curves revealed that the curves conformed to a second order polynomial of the form:

$$\ln (D_f/D_0) = B_0 + B_1 \ln (H_0/H_f) + B_2 [\ln (H_0/H_f)]^2 \dots\dots\dots(4)$$

Where, ‘B₀’, ‘B₁’ and ‘B₂’ are found to be empirically determined constants and are dependent upon the initial aspect ratios and alloy compositions. These constants along with the values of the regression coefficients are given in Table 5. Observing this table carefully, it is, found that the constant ‘B₀’ is virtually negligible and small, and, therefore, can be taken to be practically zero and can be taken off from the above polynomial because at no deformation, there is no diameter strain with respect to height strain. The constant ‘B₁’ is generally positive and contributes to linear increase in the diameter strain with respect to height strain, but, ‘B₂’ being always positive and multiplied by the square of the height strain giving rise to a parabolic increase, but, in

the final stages, the curves tended to be almost parallel to the theoretical line conforming to a positive fact that in the final stages of

Table 5 The Coefficients of the Second Order Polynomial of the Form: $[\ln (D_f/D_o)] = B_0 + B_1 \ln (H_o/H_f) + B_2 \{ \ln (H_o/H_f) \}^2$ for Iron and AISI 3115 Steel During Hot Deformation.

System	Aspect Ratio	B ₀	B ₁	B ₂	R ²
Iron	0.6	-0.002	0.12	0.312	0.999
	0.85	-0.007	0.158	0.278	0.995
	1.05	-0.006	0.192	0.233	0.993
AISI 3115	0.6	-0.008	0.193	0.273	0.994
	0.85	-0.004	0.109	0.322	0.998
	1.05	-0.021	0.098	0.309	0.998

Upsetting mode of deformation, the flow of the material and the pores became almost simultaneous. Now analyzing the regression coefficients whose values are found to be extremely close to unity indicating that the empirical equation arrived at, is justified and is valid under the boundary conditions of deformations, i.e., presuming that absolutely, too, little or absolutely, too, high strains are not induced. In, too, little deformations, the effect of true diameter strain and the true height strain is neglected and also inducing, too, high strains would be leading to circumferential crack formations which would result in a deceptive outcome. Therefore, in the nutshell, the equation relating the true diameter strain and the true height strain is given as underneath:

$$\ln (D_f/D_o) = B_1 \ln (H_o/H_f) + B_2 [\ln (H_o/H_f)]^2 \dots\dots\dots(5)$$

3.2 Deformation, Densification and Poisson’s Ratio

Figs. 4 (a) and 4 (b) show the variation between Poisson’s ratio (v_p) and the percentage theoretical density $\{ \% (\rho_f/\rho_{th}) \}$ during hot upset forging of sintered preforms of Iron and AISI 3115 P/M steel respectively. General observations of these curves shown in these figs. 4 (a) and 4 (b) are found to be very much similar to each other. There is a very clear distinction that the curves corresponding to the largest aspect ratio preforms is on the top of all the curves and the curves representing the minimum aspect ratio preforms positioned themselves at the bottom of all other aspect ratio curves. However, the curves representing to the middle aspect ratio preforms remained in the middle of above two curves. It is, also observed from these curves starting from around 92% density till around 98% density, the Poisson’s ratio has gone up quite slowly with an increased level of densification, and, thereafter

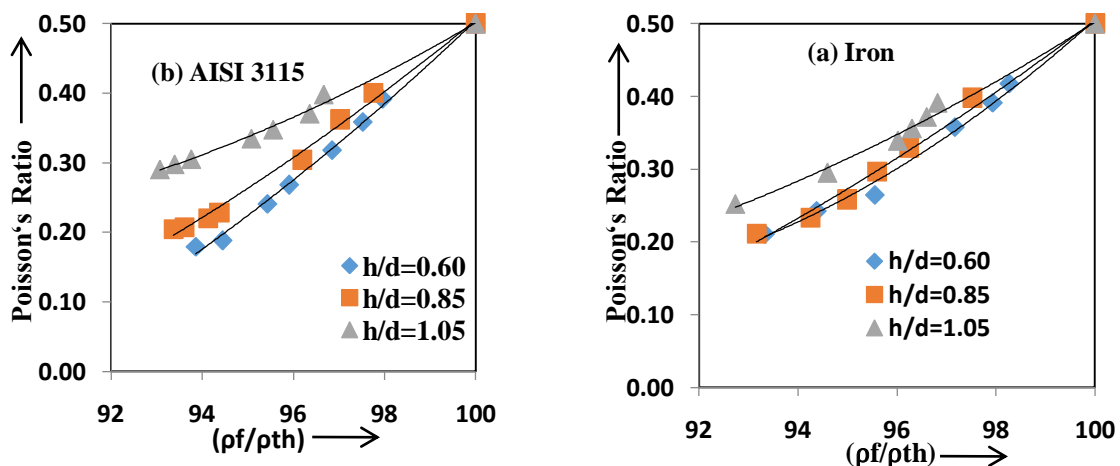


Figure 4 Relationship between Poisson’s Ratio and Percentage Theoretical Density during Hot Upset Forging of Sintered (a) Iron Preforms and (b) AISI 3115 P/M Steel Preforms

The rate of densification has been low with high rise in the values of the Poisson’s ratio. It is further noted that in the near vicinity of the theoretical density, the value of the Poisson’s ratio tended to approach to a theoretically feasible value of Poisson’s ratio, i.e., 0.5. This ably supports the argument that in upset forging a cent per cent dense product cannot be achieved and, hence, the limiting value of Poisson’s ratio of 0.5 is not approached. The curves drawn in figs. 4 (a) and 4 (b) on analysis have revealed that an empirical relationship

between Poisson’s ratio and the percentage theoretical density conformed to a second order polynomial of the form as is given below:

$$v_p = C_0 + C_1 \{ \%(\rho_f/\rho_{th}) \} + C_2 \{ \%(\rho_f/\rho_{th}) \}^2 \dots\dots\dots (6)$$

Where, the coefficients of the second order polynomial given in equation 6 are ‘C₀’, ‘C₁’ and ‘C₂’ respectively and they are found to depend upon the compositions of the systems and the preform geometries of the preforms. The values of these constants ‘C₀’, ‘C₁’ and ‘C₂’ for both the systems along with the values of regression coefficient ‘R²’ are given in Table-6. The values of ‘R²’ are found to be in close vicinity of unity. It is, therefore, clearly established that the relationship empirically arrived at stands ably justified

Table 6 The Coefficients of the Second Order Polynomial of the Form: Poisson’s Ratio (v_p) = C₀ + C₁ { (%(ρ_f/ρ_{th})) + C₂ { (%(ρ_f/ρ_{th}))² for Sintered Iron and AISI 3115 P/M Steel Preforms during Hot Upset Deformation.

System	Aspect Ratio	C ₀	C ₁	C ₂	R ²
Iron	0.6	15.7	-0.366	0.002	0.995
	0.85	-9.13	0.145	0.001	0.989
	1.05	-2.379	0.017	0.001	0.99
AISI 3115	0.6	-43.18	0.836	0.004	0.992
	0.85	-19.22	0.357	0.001	0.997
	1.05	-28.66	0.565	0.002	0.99

3.3 Deformation, Densification and Bulging

Figs. 5 (a) and 5 (b) have been drawn between percent theoretical density attained and the bulging ratio for both the systems investigated in the present work. The characteristic nature of the curves drawn in these two figs. 5(a) and 5(b) stand quite similar to each other and when analytically analyzed were found to be in close conformity with a second order polynomial of the form as stated below:

$$\{ \%(\rho_f/\rho_{th}) \} = E_0 + E_1 (D_b/D_0) + E_2 (D_b/D_0)^2 \dots\dots\dots (7)$$

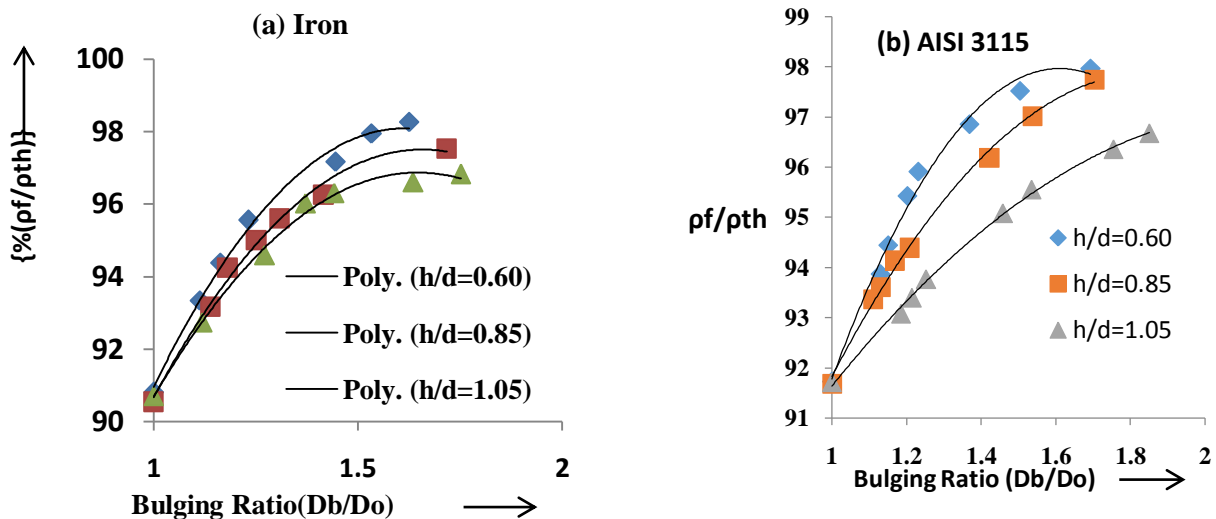


Figure 5 Relationship between percent Fractional Theoretical Density and Bulging Ratio during Hot Upset Forging of Sintered AISI 3115 Preforms.

Where, ‘E₀’, ‘E₁’ and ‘E₂’ are empirically determined constants and are found to depend upon the preform geometries and the systems compositions. The values of these coefficients. i.e., ‘E₀’, ‘E₁’ and ‘E₂’ along with the values of the regression coefficient ‘R²’ are listed in Table-7. Observing the values of the regression coefficient ‘R²’, it is found that they are in close proximity to unity and hence the expression { % (ρ_f / ρ_{th}) } = E₀ + E₁ (D_b/D₀) + E₂ (D_b/D₀)² empirically arrived at stands technically validated.

Table 7 The Coefficients of the Second Order Polynomial of the Form $(\% \rho_f / \rho_{th}) = E_0 + E_1 (D_b/D_0) + E_2 (D_b/D_0)^2$ for Iron and AISI 3115 Steel during Hot Deformation.

System	Aspect Ratio	E ₀	E ₁	E ₂	R ²
Iron	0.6	43.64	69.79	-22.34	0.989
	0.85	45.06	66.72	-21.22	0.991
	1.05	56.31	49.5	-15.1	0.993
AISI 3115	0.6	53.14	55.94	-17.43	0.99
	0.85	66.37	35.46	-10.03	0.995
	1.05	78.13	17.58	-4.093	0.996

3.4 Deformation, Densification and Power Law Relationship

Figs. 6 (a) and 6 (b) have been drawn between logarithm of per cent theoretical density and the logarithm of bulging ratio for both the systems that were investigated in the present study. It has been found that straight lines continuous or in two segments were found to be well represented by the calculated parameters such as percent theoretical density and the bulging ratio. These plots show that a relationship of the form given below:

$$\text{Log } \{ \% (\rho_f / \rho_{th}) \} = m \log (D_b / D_0) + Q \dots \dots \dots (8)$$

The above expression when simplified represents a power law equation of the form as given underneath:

$$(\rho_f / \rho_{th}) = Q_0 (D_b / D_0)^m \dots \dots \dots (9)$$

Where, the constants ‘Q’ and ‘m’ are found to be empirically determined constants depending upon the values of initial preform geometries and the composition. However, one interesting aspect which can be observed from Table 8 where the constants ‘Q’ and ‘m’ are listed is that for a given aspect ratio in a given segment the values of ‘m’ keeps decreasing while the values of ‘Q’ remaining more or less constant. The values of the regression coefficient ‘R²’ is found to be very much in close vicinity of unity and, therefore, the expression proposed in the equation (7) is justified and the values of the constants including the values of ‘R²’ are listed in Table 8 which determine the rapidity to an increase in per cent theoretical density on deformation and the resultant increase in bulging.

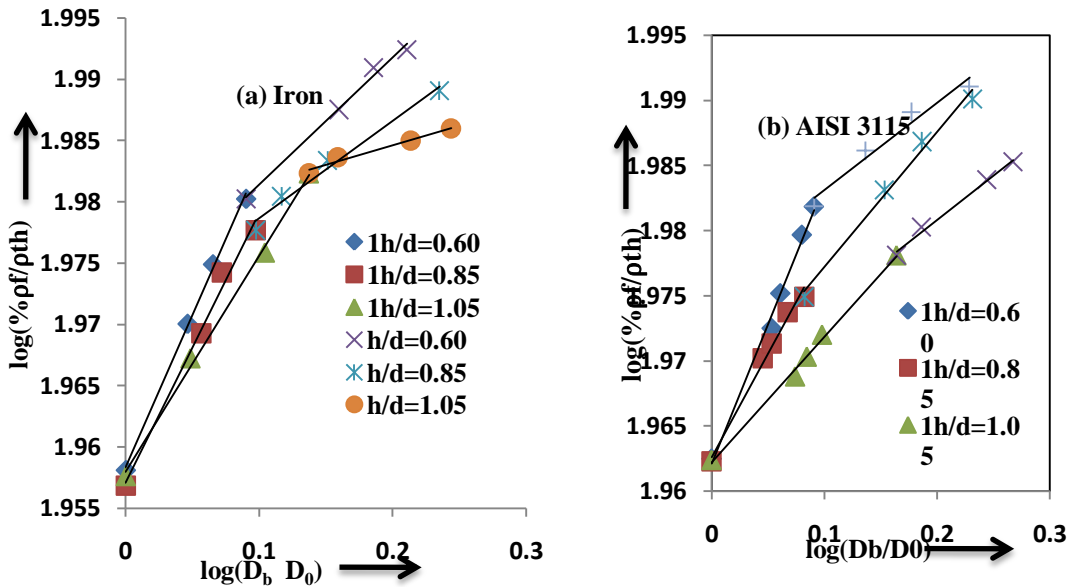


Figure 6 Relationship between Log (% Fractional Theoretical Density) and log (Bulging Ratio) during Hot Upset Forging of Sintered Preforms of (a) Iron and (b) AISI 3115 P/M Steel Preforms.

Table 8 The Slope and Intercepts of the of the Form $\text{Log}\{\%(\rho_f/\rho_{th})\} = m\text{Log}(\%D_b/D_o) + Q$ for Iron and AISI 3115 Steel During Hot Deformation.

System	Aspect Ratio	m	Q	R ²
Fe	0.6	0.247	1.958	0.998
	0.85	0.22	1.957	0.99
	1.05	0.176	1.958	0.997
	0.6	0.104	1.971	0.992
	0.85	0.079	1.97	0.991
	1.05	0.032	1.97	0.993
AISI 3115	0.6	0.223	1.961	0.99
	0.85	0.158	1.962	0.989
	1.05	0.096	1.962	0.996
	0.6	0.058	1.977	0.99
	0.85	0.103	1.966	0.989
	1.05	0.067	1.967	0.993

IV. Conclusions

Based on the experimental data and calculated parameters and their analysis critically carried out has yielded the major findings of the present investigation are given as underneath:

- Rate of densification has been established as a function of preform geometries and the compositions of the systems investigated. Lower aspect ratio preforms have been found to densify at a much faster rates compared to the larger aspect ratio preforms due to rapid and uniform load transfer across the axial direction which is caused due to lower pore bed depth. The relationship between fractional theoretical density (ρ_f/ρ_{th}) and the true height strains is given as beneath:

$$(\rho_f/\rho_{th}) = A_0 + A_1 \ln(H_o/H_f) + A_2 [\ln(H_o/H_f)]^2$$

Where, (ρ_f/ρ_{th}) is the fractional theoretical density, $\ln(H_o/H_f)$ is representing the true height strain, and, 'A₀', 'A₁' and 'A₂' are empirically determined constants. The constant 'A₁' played a major role in enhancing the densification rate especially in the lower range of height strains. The constant 'A₀' did not contribute to densification as the same has been constant and equal to the initial preform densities, but, the constant 'A₂' contributed mainly towards flattening the curves in the final stages of deformation and densification as all its values for each aspect ratios were negative, but, of low magnitude,

- All data points corresponding to plots representing the true diameter strain and the true height strains have been found to lie below the theoretical line with a slope of 0.5 conforming that the values of the Poisson's ratio would tend to approach to a value of 0.5, but, would never reach it. This is true irrespective of the preform geometry and the alloying compositions considered in the present investigation. The curves corresponding to the above strains have well conformed to a second order polynomial of the form:

$$\ln(D_f/D_o) = B_0 + B_1 \ln(H_o/H_f) + B_2 [\ln(H_o/H_f)]^2$$

Where, $\ln(D_f/D_o)$ is true diameter strain and $\ln(H_o/H_f)$ is true height strain.

- The relationship between the Poisson's ratio and the per cent fractional theoretical density was established to conform to a second order polynomial of the form as given underneath:

$$v_p = C_0 + C_1 \{\%(\rho_f/\rho_{th})\} + C_2 \{\%(\rho_f/\rho_{th})\}^2$$

Where, v_p is the Poisson's ratio, $\{\%(\rho_f/\rho_{th})\}$ is percentage fractional theoretical density attained at a given deformation and 'C₀', 'C₁' and 'C₂' are empirically determined constants depending upon initial preform geometry and the composition. There are two modes of densification which is clearly observed and one of them is a region of slow rise of Poisson's ratio with maximum densification and the other one is the steep rise in the values of Poisson's ratio with lesser degree of densification corresponded to a situation where pore and material flow became almost simultaneous meaning thereby that the pores have thermodynamically got stabilized. Hence, the above relationship is ably justified

- Definite relationships between fractional theoretical density (ρ_f/ρ_{th}) and the bulging ratio have been found and the same conformed to a second order polynomial of the form given below:

$$(\rho_f/\rho_{th}) = E_0 + E_1 (D_b/D_o) + E_2 (D_b/D_o)^2$$

Where, 'E₀', 'E₁' and 'E₂' are empirically determined constants and established to depend upon the initial preform geometries and the compositions of the systems investigated.

- A power Law relationship between per cent fractional theoretical density and the bulging ratio have been established which covered the two different density zones of fractional theoretical densities and the two different regions of the Poisson's ratio and the same is given as under:

$$\{\% \rho_f/\rho_{th}\} = Q_0 (D_b/D_o)^m$$

Where, ' Q_0 ' and ' m ' are empirically determined constants which were found to depend upon the initial preform geometries and the compositions of the systems investigated.

REFERENCES

- [1]. Anil Kumar Sinha, "Powder Metallurgy", Dhanpat Rai Publications (P) Ltd. 1987.
- [2]. Syed Ummer M. Thangal, K. S. Pandey, C. Natarajan and S. Shanmugam, "Ring Fracture strength and Hardness in Sintered Hot Deformed High Carbon Steel Preforms", International Journal of Materials Science, Vol. 3, No. 1, pp. 75-88, 2008.
- [3]. Ryuichiro Goto, "Powder Metallurgy Growth in Automotive Market", In: Business Briefing: Global Automotive Manufacturing and Technology, Materials, London, UK, pp. 44-45, 2007.
- [4]. Rober. J. Causton and Christophere. Schade, "Machinability: Material Property or Process Response", Hoeganaes Corporation, Cimanamission, NS08077, Presented at PMTEL, Las Vegas, 2003.
- [5]. Rajesh Kannan, K. S. Pandey, S. Shanmugam and R. Narayanasamy, "Sintered Fe-0.8%C-1.0%Si-0.4%Cu P/M steel Preform Behaviours During Cold Upsetting", Journal of Iron and Steel Research, International, Vol. 15 (5), pp. 81-87, 2008.
- [6]. Dhanasekaren and R. Ganamoorthy, "Microstructure Strength and Tribological Behaviour of Fe-C-Cu-Ni Sintered Steel Prepared with MoS₂ Addition", Journal Materials Science, Vol. 42, pp. 4659-4666, 2007.
- [7]. K.S.Pandey and R. Vijayaraghavan, " Extrusion Forging of Indigenously Developed Iron- 0.25% Phosphorous Alloy Powder Preforms in Different Die Cavities", Quarterly International Journal of Powder Metallurgy Science and Technology, Vol.6 ,No.4, pp. 8-18, 1995.
- [8]. T. Kimura and H. Hamamoto, "Strengthening of Iron Compacts by Infiltration", Modern Developments in Powder Metallurgy, Vol. 8, pp.135-147, 1974.
- [9]. R. Chandramouli, T. K. Kandavel, D. Shanmugasundaram and T. Ashok Kumar, "Deformation, Densification and Corrosion Studies of sintered Power Metallurgy Plain carbon Steel Preforms", Materials and Design, Vol. 28, pp. 2260-2264, 2008.
- [10]. H. A. Kuhn and A. Lawley, "Powder Metallurgy Processing New Techniques", Academic Press, New York, pp. 99-138, 1978.
- [11]. J. Wisker and P.K. Jones, "The Economics of Powder Forging Relative to Competing: Process Present and Future", Modern Developments in Powder Metallurgy, Vol. 7, pp. 33-49, 1974.
- [12]. K. S. Pandey. "Salient Characteristics of High Temperature Forging of Ferrous Preforms", Key Engineering Materials, Switzerland: Trans. Tech. Publications, pp. 465-486, 1989.
- [13]. Halter. R.F, "Recent Advances in the Hot Forming of P/M Preforms", Modern Developments in Powder Metallurgy, Edited by; Hausner, H.H, Smith W.E, Vol.7, pp.137-152, 1974.
- [14]. Torre's Model (C. Huttenmannische Montsh, Vol. 93, pp. 62, 1948) as Quoted by K.S.Pandey in his Ph.D. Thesis entitled "Densification Behaviour of Iron and Iron Based Alloy Powder Preforms During Hot Forging" at University of Roorkee (now IIT Roorkee) August 1982.
- [15]. Olle Grinder, Caoyoung Jia and Lyla Nisson, "Hot Upsetting and Hot Repressing of Sintered Steel Preform", Modern Developments in Powder Metallurgy, Vol. 15, pp. 33-49, 1982.
- [16]. K.S. Pandey, "Modified Indigenous High Temperature Coating", REC Trichy, 1986.
- [17]. Moyer K.H, "Measuring Density of P/M Materials with Improved Precision", International Journal of Powder Metallurgy and Powder Technology, Vol. 15, pp. 33-42, 1979.